

Generation of quasi-monoenergetic electron beams using ultrashort and ultraintense laser pulses*

Y. GLINEC,¹ J. FAURE,¹ A. PUKHOV,² S. KISELEV,² S. GORDIENKO,² B. MERCIER,¹
AND V. MALKA¹

¹Laboratoire d'Optique Appliquée, Ecole Polytechnique, ENSTA, CNRS, UMR, Palaiseau, France

²Institut für Theoretische Physik, Heinrich-Heine-Universität Duesseldorf, Duesseldorf, Germany

(RECEIVED 1 October 2004; ACCEPTED 13 December 2004)

Abstract

Plasma-based accelerators have been proposed for the next generation of compact accelerators because of the huge electric fields they can support. However, it has been difficult to use them efficiently for applications because they produce poor quality particle beams with large energy spreads. Here, we demonstrate a dramatic enhancement in the quality of electron beams produced in laser-plasma interaction: an ultrashort laser pulse drives a plasma bubble which traps and accelerates plasma electrons to a single energy. This produces an extremely collimated and quasi-monoenergetic electron beam with a high charge of 0.5 nanocoulomb at energy 170 ± 20 MeV.

Keywords: Laser-plasma accelerator; Monoenergetic electron beam; Ultrashort electron beam; Ultrashort laser-plasma interaction

1. INTRODUCTION

Particle accelerators are used in a tremendous variety of fields, ranging from medicine (for medical imaging and radiotherapy) to high energy physics, and inertial fusion applications (Tahir *et al.*, 2004). Electron accelerators, such as synchrotrons, are used as radiators for generating light sources from the X-ray to the far-IR region (Alesini *et al.*, 2004). Here again, these light sources find a wide variety of applications ranging from THz imaging to X-ray diffraction on biological samples. A conventional accelerator is usually composed of a seed particle beam which is fed into radio frequency accelerating structures. However, this technology is reaching a bottleneck because the accelerating fields are limited to 50 MV/m due to material breakdown, which occurs on the walls of the structure. Thus, high energy accelerators tend to be expensive and large scale infrastructures, which can be prohibitive for some applications (Hoffmann *et al.*, 2005). In this context, plasma-based accelerators (Tajima & Dawson, 1979) are of great interest because of their ability to sustain extremely high acceleration gradients, in excess of 100 GV/m. Such high fields make plasma-

based accelerators likely candidates for the next generation of compact accelerators (Nakajima, 2000; Malka, 2002; Weber *et al.*, 2004).

For most practical applications, high quality particle beams with high spatial quality and monoenergetic energy distribution are required. A beam which does not satisfy these criteria would be hard to use because it would be almost impossible to transport it and/or to focus it.

In order to produce high quality beams from plasma-based accelerators, two challenges have to be met: (1) generation of an accelerating structure in the plasma, (2) production of a high quality seed beam and its injection into the accelerating structure.

The generation of accelerating structures in plasmas relies on the excitation of large amplitude plasma waves by a focused ultra-intense laser. One possible mechanism is the excitation of plasma waves by the laser ponderomotive force. When the laser pulse length $c\tau$ (where c is the speed of light and τ is the pulse duration) is comparable to the plasma wavelength λ_p , the ponderomotive force, which is proportional to the gradient of the laser envelope, efficiently pushes plasma electrons out of the region where the laser field is strong. The plasma ions, much heavier, stay on, creating the space charge separation field needed for particle acceleration, that is, the plasma wave. The phase velocity of the space charge field is the laser group velocity, which is close

Address correspondence and reprint requests to: Jérôme Faure, LOA, Chemin de la Hunière, 91761 Palaiseau, France. Email: jerome.faure@ensta.fr

*This paper was presented at the 28th ECLIM conference in Rome, Italy.

to c , making the plasma wave suitable for relativistic particle acceleration.

The generation of intense accelerating fields in plasmas has been demonstrated in many experiments (Clayton *et al.*, 1985; Kitagawa *et al.*, 1992; Amiranoff *et al.*, 1992). Proof-of-principle experiments have shown the feasibility of externally injecting electrons from a conventional accelerator into the laser-driven plasma accelerating structure (Kitagawa *et al.*, 1992; Everett *et al.*, 1994; Dorchiès *et al.*, 1999). However, the output beam quality has been poor: the electron energy distribution has had a 100% energy spread. The production of monoenergetic beams with this method puts stringent constraints on the injector: electrons have to be injected in a particular phase of the plasma wave, which implies injecting a sub-100 fs electron bunch. The technology for producing such short bunches containing a high charge does not exist yet. Currently, the most widespread method for producing electron beams from plasmas relies on the self-modulated laser wake field (SMLWF) accelerator (Andreev *et al.*, 1992; Sprangle *et al.*, 1992; Antonsen & Mora, 1992). In this scheme, the laser pulse is longer than the plasma wavelength. Under the influence of the self-modulation instability, its envelope modulates at the plasma frequency. The ponderomotive force associated to the modulated envelope is then able to resonantly excite a plasma wave. However, this mechanism cannot be controlled because it relies on an instability. Thus, the laser modulates more severely as the plasma wave amplitude grows. When the amplitude reaches the wave breaking level, copious amounts of plasma background electrons are trapped in the plasma wave and accelerated, subsequently destroying the plasma wave itself. Numerous experiments report on the production of electron beams with nC charge and divergence varying from a few degrees to tens of degrees and Maxwellian energy distributions (Modena *et al.*, 1995; Umstadter *et al.*, 1996a; Moore *et al.*, 1997). More recently, several groups (Gahn *et al.*, 1999; Malka *et al.*, 2001) demonstrated that more compact lasers with high repetition rates can be used to generate high repetition rate (10 Hz) electron sources, which could be used for applications. Using these compact and short pulse lasers, it has been shown that electrons can be accelerated up to 200 MeV (Malka *et al.*, 2002) with an improved spatial beam quality (Fritzler *et al.*, 2004). However, these beams still have very large energy spread and a low number of electrons at high energy (typically <1 pC at $200 \text{ MeV} \pm 10 \text{ MeV}$).

The limited beam quality was inherent to previous experiments: wavebreaking occurred under the laser pulse envelope and the accelerated electrons were also under the influence of the ultra intense laser field. Direct laser acceleration (Pukhov *et al.*, 1999; Gahn *et al.*, 1999; Shorokov & Pukhov, 2004) by transverse laser field deteriorated the spatial beam quality, causing emittance growth. In order to circumvent the problems caused by wave breaking, schemes involving several laser pulses have been proposed (Umstadter *et al.*, 1996b; Esarey *et al.*, 1997): one laser pulse is used to

generate a plasma wave while the other ensures injection in a given region of phase space for monoenergetic acceleration. However, the difficulties associated with such complicated experiments have not yet permitted the production of high quality beams.

2. EXPERIMENT

In this paper, we demonstrate the generation of high quality electron beams from the interaction of a single beam with under dense plasma. Extremely collimated beams with 10 mrad divergence and 0.5 nC (± 0.2 nC) of charge at $170 \text{ MeV} \pm 20 \text{ MeV}$ have been demonstrated. Contrary to all previous results obtained from laser-plasma accelerators, the electron energy distribution is quasi-monoenergetic (Faure *et al.*, 2004). The number of high energy electrons (170 MeV) is increased by at least three orders of magnitude with respect to previous work. This high performance was obtained in a new acceleration regime: a single laser beam was used to generate a highly nonlinear wakefield (resembling a plasma bubble), able to trap and accelerate plasma electrons to high energy.

Monoenergetic electron acceleration in a plasma bubble was recently discovered using computer simulations of laser-plasma interaction (Pukhov & Meyer-ter-Vehn, 2002). The formation of a plasma bubble is optimized when the plasma is fully resonant with the laser pulse, that is, when the transverse and longitudinal dimensions of the laser pulse are about the plasma wavelength. In this case, the laser ponderomotive force expels all electrons violently, creating a cavity (or plasma bubble) around the laser pulse. This is referred to as the “blow-out” regime (or cavitation). The cavity carries very high electric fields, on the order of the wave breaking field $E_0 = 2\pi m_e/e\lambda_p$, where m_e and e are, respectively, the electron mass and charge ($E_0 = 100 \text{ GV/m}$ for a $n_e = 10^{18} \text{ cm}^{-3}$ electron plasma density). In spite of these extremely high fields, the cavity maintains its structural integrity and propagates as long as the laser intensity stays high. Thus, the cavity is able to trap electrons and to accelerate them to high energies over mm lengths. As electrons dephase with respect to the accelerating fields, they tend to self-bunch and form a monoenergetic peak in energy.

This regime has been reached by using the ultrashort and ultra intense laser pulse generated in a titanium doped sapphire, chirped pulse amplification laser system (Strickland & Mourou, 1985). The laser pulse had a 30 fs duration at full width half maximum (FWHM), contained 1 J of laser energy at central wavelength 820 nm (Pittman *et al.*, 2002). It was focused onto the edge of a 3 mm long supersonic helium gas jet using an f/18 off-axis parabola. The diffraction limited focal spot was $r_0 = 21 \mu\text{m}$ at FWHM, producing vacuum-focused laser intensity of $I = 3.2 \times 10^{18} \text{ W/cm}^2$, for which the corresponding normalized potential vector is $a_0 = eA/(mc^2) = 1.26$. For these high laser intensities, the helium gas was fully ionized by the foot of the laser pulse.

Monoenergetic electron distributions were observed for densities of $n_e = 6 \times 10^{18} \text{ cm}^{-3}$, for which the plasma wavelength ($\lambda_p = 13.6 \text{ }\mu\text{m}$) is comparable to the laser pulse length ($c\tau = 9 \text{ }\mu\text{m}$). The diameter ($r_0 = 21 \text{ }\mu\text{m}$) was larger than the plasma wavelength, but one may expect that self-focusing in the plasma brings it down to the matched value.

As shown on Figure 1, electron detection was achieved using a LANEX phosphor screen. As electrons passed through the screen, energy was deposited and reemitted into visible photons, which were then imaged onto a 16 bit charged coupled device (CCD) camera. When inserting a magnet, electrons were deflected and the image on the screen represented the electron energy distribution. The total beam charge was measured using an integrating current transformer (ICT), placed about 30 cm behind the LANEX screen.

Figure 2 shows a picture of the electron beam when no magnetic field is applied. The electron beam is very well collimated with a 5–10 mrad divergence at FWHM, the smallest divergence ever measured for a beam emerging from a plasma accelerator. One can explain this low divergence using several arguments: (1) electrons are accelerated in the plasma bubble but they stay behind the laser pulse and do not interact with its defocusing transverse field, (2) when electrons exit the plasma, their energy is very high and therefore, the effect of space charge is greatly diminished. Figure 3 shows the deviation of the beam when a magnetic field is applied. The images show how the electron spectrum evolves when the plasma density is changed. It is possible to obtain quasi-monoenergetic distributions for low density

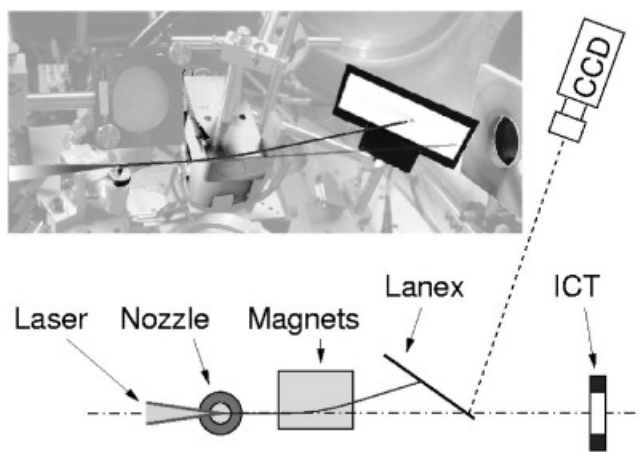


Fig. 1. Experimental set-up. Top: picture from the experiment, bottom: schematic. An ultrashort and ultra intense laser pulse is focused onto a 3 mm supersonic gas jet and produces a very collimated 170 MeV electron beam. Electrons are detected using a LANEX phosphor screen, imaged onto a 16 bit CCD camera. The charge of the electron beam is measured using an integrating current transformer (ICT). For energy distribution measurements, a 0.45 Tesla, 5 cm long permanent magnet is inserted between the gas jet and the LANEX screen. The LANEX screen is protected by a 100 μm thick aluminum foil in order to avoid direct exposure to the laser light.

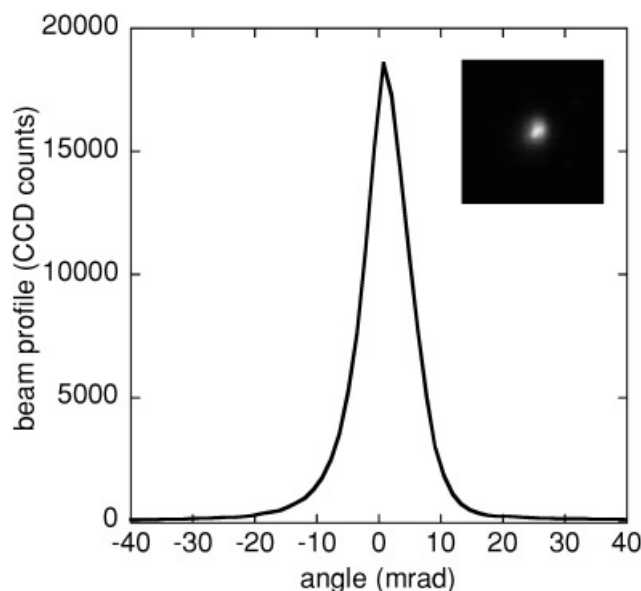


Fig. 2. Electron beam profile. Insert: image obtained on the LANEX screen. Graph: horizontal cut.

plasmas: at $n_e = 6 \times 10^{18} \text{ cm}^{-3}$, the spectrum exhibits a narrow peak around 170 MeV, indicating efficient monoenergetic acceleration. For comparison, at higher density ($n_e = 2 \times 10^{19} \text{ cm}^{-3}$), electrons are accelerated to all energies but the number of high energy electrons is low. In addition, the beam divergence is much larger than for the low density cases.

Figure 4 shows an electron spectrum after deconvolution. The spectrum clearly shows a quasi-monoenergetic distribution peaked at 170 MeV, with a 24% energy spread (at FWHM). This peaked energy distribution is a clear signature of the formation of a plasma bubble as seen in computer simulations (Pukhov & Meyer-ter-Vehn, 2002).

Finally, the charge contained in this bunch can be inferred using the ICT. Without the magnet, the whole beam charge measured on the ICT is $2 \pm 0.5 \text{ nC}$. The ICT signal can be correlated to the LANEX images to infer the charge at high energy. This shows that the charge at $170 \text{ MeV} \pm 20 \text{ MeV}$ is $0.5 \text{ nC} \pm 0.2 \text{ nC}$. From the above, one can deduce that the electron beam energy was 100 mJ, so that the energy conversion from the laser to the electron beam was about 10%.

Experimentally, this regime could be reached in a very narrow range of parameters: stretching the pulse duration above 50 fs was sufficient to loose the peaked energy distribution. Similarly, when the electron density was increased from $6 \times 10^{18} \text{ cm}^{-3}$ to $7.5 \times 10^{18} \text{ cm}^{-3}$, the energy distribution became a broad plateau, similar to results obtained in the forced laser wakefield regime (Malka *et al.*, 2002). Above 10^{19} cm^{-3} , the electron distribution was Maxwellian-like with very few electrons accelerated at high energy. Below $6 \times 10^{18} \text{ cm}^{-3}$, the number of accelerated electrons decreased dramatically. The evolution of electron spectra with experimental parameters indicates that using laser pulses

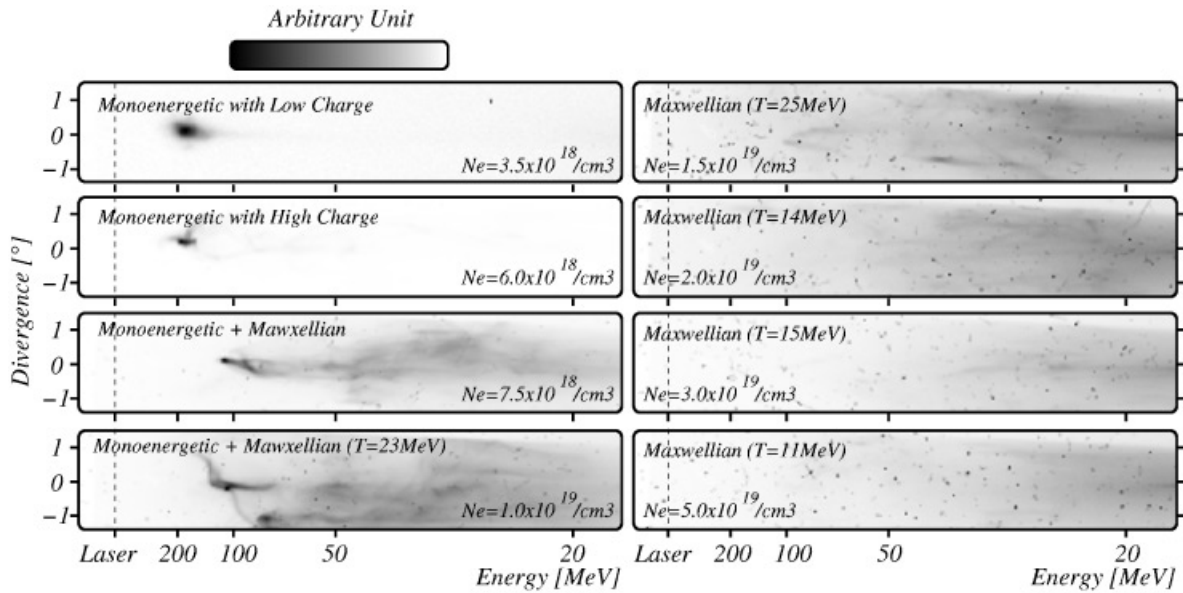


Fig. 3. Raw images obtained on the LANEX screen. The vertical dashed line is drawn at the intersection of the laser axis with the LANEX screen. The images show the transition from a monoenergetic well-collimated electron beam (for $n_e = 3.5 \times 10^{18} \text{ cm}^{-3}$ and $6 \times 10^{18} \text{ cm}^{-3}$) to a beam with a spectrum with a plateau (for $n_e = 7.5 \times 10^{18} \text{ cm}^{-3}$ and 10^{19} cm^{-3}) and finally to a Maxwellian spectrum (for $n_e > 1.5 \times 10^{19}$).

shorter than the plasma period is beneficial to high quality and monoenergetic electron acceleration. It should also be noted that the use of a larger spot size was crucial to the success of the experiment: when using a shorter focal length parabola ($f = 30 \text{ cm}$ instead of $f = 1 \text{ m}$) and a smaller spot

size, it was impossible to obtain monoenergetic beams. In particular, it was impossible to generate an electron beam for densities smaller than 10^{19} cm^{-3} . We believe this is because the use a larger spot size insures a longer interaction length with high laser intensity.

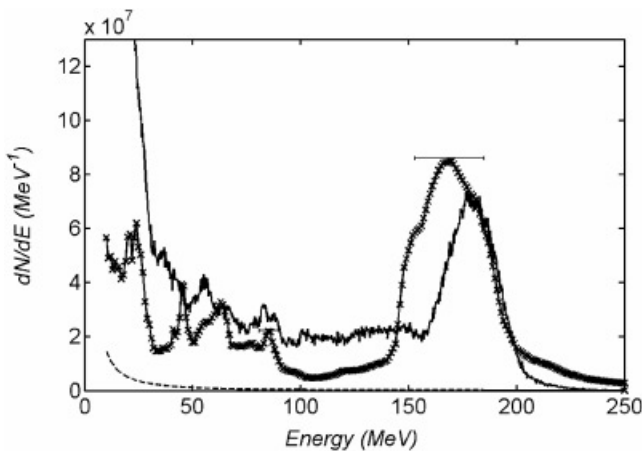


Fig. 4. Electron spectrum corresponding to Fig. 3 at $n_e = 6 \times 10^{18}$, after deconvolution (line with crosses). The dashed line represents an estimation of the background level. For deconvolution, electron deviation in the magnetic field has been considered as well as the electron stopping power inside the LANEX screen. The horizontal error bars indicate the resolution of the spectrometer for different energies. The resolution is limited by the electron beam spatial quality as well as by the dispersing power of the magnet. This gives a resolution of respectively 32 MeV and 12 MeV for 170 MeV and 100 MeV energies. Above 200 MeV, the resolution quickly degrades. The full line is the electron spectrum obtained from 3D PIC simulations.

3. PIC SIMULATIONS

To reach a deeper understanding of the experiment, we ran three-dimensional particle-in-cell (PIC) simulations using the code from the Virtual Laser Plasma Laboratory (Pukhov, 1999). The simulation results are shown in Figure 5a, 5b, and 5c. The simulation suggests that our experimental results can be explained by the following scenario. (1) At the beginning of the simulation, the laser pulse length ($9 \mu\text{m}$) is nearly resonant with the plasma wave ($\lambda_p = 13.6 \mu\text{m}$); but its diameter ($21 \mu\text{m} > \lambda_p$) is larger than the matched one. (2) As the pulse propagates in the plateau region of the gas jet, it self-focuses and undergoes longitudinal compression by plasma waves, Figure 5a. This decreases the effective radius of the laser pulse and increases the laser intensity by one order of magnitude. (3) This compressed laser pulse is now resonant with the plasma wave and it drives a highly nonlinear wakefield, Figure 5b: the laser ponderomotive potential expels the plasma electrons radially and leaves a cavitated region behind. In this regime, the three-dimensional structure of the wakefield resembles a plasma bubble. (4) As the electron density at the walls of the bubble becomes large, and electrons are injected and accelerated inside the bubble. (5) As the number of trapped electrons increases, the bubble elongates. Its effective group velocity decreases and elec-

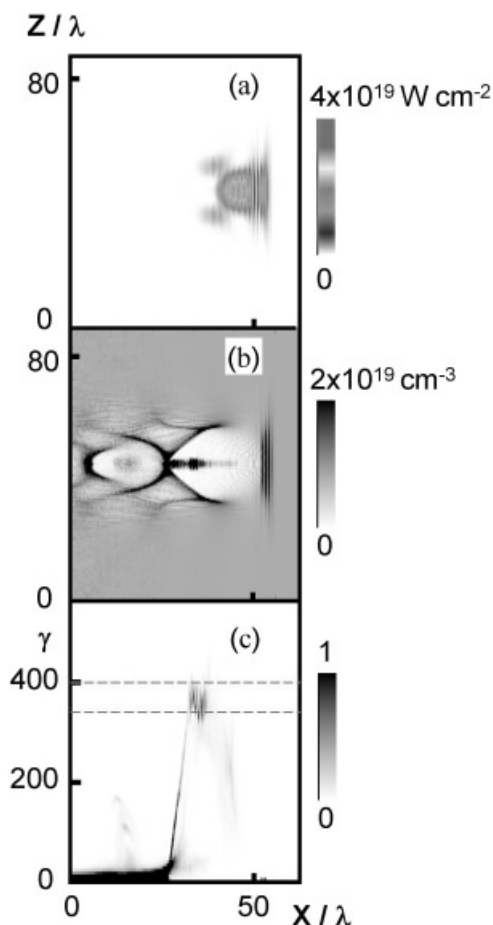


Fig. 5. 3D PIC simulation results. **a, b,** Distributions of laser intensity (**a**) and electron density (**b**) in the x - z -plane, which is perpendicular to the polarization direction and passes through the laser axis. The laser pulse runs from left to right, and has propagated 2 mm in the plasma. The bubble structure is clearly visible. The laser pushes the electron fluid forward at the bubble head and creates a density compression there. Behind the laser we see the cavitated region with nearly zero electron density. The radically expelled electrons flow along the cavity boundary and collide at the X-point at the bubble base. Some electrons are trapped and accelerated in the bubble. The beam of accelerated electrons is seen as the black rod in **b**. These electrons are propagating behind the laser pulse (**a**) and are not disturbed by the laser field. **c,** Electron phase space density $f(x, \gamma)$ in arbitrary units. We see that the electrons have dephased and have self-bunched in the phase space around $\gamma \gg 350$.

trons start to dephase with respect to the accelerating field. This dephasing causes electron self-bunching in the phase space, Figure 5c. This self-bunching results in the monoenergetic peak in the energy spectrum, see Figure 4. The appearance of the monoenergetic peak in the electron energy distribution comes from the complex interplay between electron injection in the bubble, dephasing and changes in the bubble structure during propagation (both the electric fields and the effective group velocity change during propagation).

Simulations also show that the quality of the electron beam is higher when trapped electrons do not interact with

the laser field. If this were to occur, the laser field would cause the electrons to scatter in phase space, degrading the low divergence as well as the monoenergetic distribution. This argument could explain why higher quality beams are obtained experimentally for shorter pulses and lower electron densities.

Figure 5a shows that the self-focused and compressed laser pulse stands in front of the trapped electrons (Fig. 5b), leaving them almost undisturbed. The electron energy spectrum obtained from the simulations is shown on Figure 4: it peaks at 175 ± 25 MeV, in agreement with the experiment. The divergence of 10 mrad is also in agreement with experiments. Simulations also indicate that the electron bunch duration is less than 30 fs. Since the electron distribution is quasi-monoenergetic, the bunch will stay short upon propagation: considering a 24% energy spread at 170 MeV, one can show that the bunch stretches by only 50 fs/m as it propagates.

Another important point is the apparent robustness of the ‘blow-out’ regime. The initial laser parameters, for example, the focal spot radius and intensity, were far from the final values in the bubble (Fig. 5). Yet self-focusing led to compression of the laser pulse and to the formation of an electron cavity. The energy of 1 J for a 30 fs laser pulse, as used in the experiment, seems to be close to the threshold for this regime. Simulations suggest that with more laser energy and shorter pulses, the bubble regime will lead to the acceleration of monoenergetic beams at higher energies and higher charges.

4. CONCLUSION

In conclusion, by carefully selecting laser and plasma parameters, we have generated monoenergetic electron beams using a state-of-the-art laser system. These results are confirmed by 3D PIC simulations. The bunch duration (sub-30 fs), along with the present improvement on the charge (nC), and the quality of the electron beam (monoenergetic spectrum, low divergence), reinforce the major relevance of plasma-based accelerators for many applications (such as high resolution radiography for non destructive material inspection, radiotherapy, ultrafast chemistry, radiobiology, and material science). With the rapid progress of laser science, it will be possible to generate compact, monoenergetic, and high quality electron beams with a tunable energy range at a reasonable cost. This source will be perfectly adapted as an injector for future GeV laser-plasma accelerator schemes. It will also be relevant for generating ultra-short X-ray sources, using undulators or lasers via Thomson scattering.

ACKNOWLEDGMENT

We acknowledge the support of the European Community Research Infrastructure Activity under the FP6 ‘Structuring the European Research Area’ program (CARE, contract number RII3-CT-2003-506395).

REFERENCES

- ALESINI, D., BERTOLUCCI, S., BIAGINI, M.E., BONI, R., BOSCOLO, M., CASTELLANO, M., CLOZZA, A., DIPIRRO, G., DRAGO, A., ESPOSITO, A., *et al.* (2004). The SPARC/X SASE-FEL Projects. *Laser Part. Beams* **22**, 341–350.
- AMIRANOFF, F., LABERGE, M., MARQUÈS, J.-R., MOULIN, F., FABRE, E., CROS, B., MATTHIEUSSENT, G., BENKHEIRI, P., JACQUET, F., MEYER, J., MINÉ, P., STENZ, C. & MORA, P. (1992). Observation of modulational instability in Nd-laser beat-wave experiments. *Phys. Rev. Lett.* **68**, 3710–3713.
- ANDREEV, N.E., GORBUNOV, L.M., KIRSANOV, V.I., POGOSOVA, A.A. & RAMAZASHVILI, R.R. (1992). Resonant excitation of wakefields by a laser pulse in a plasma. *JETP Lett.* **55**, 571–574.
- ANTONSEN, T.M. & MORA, P. (1992). Self-focusing and Raman scattering of laser pulses in tenuous plasmas. *Phys. Rev. Lett.* **69**, 2204–2207.
- CLAYTON, C.E., JOSHI, C., DARROW, C. & UMSTADTER, D. (1985). Relativistic plasma-wave excitation by collinear optical mixing. *Phys. Rev. Lett.* **54**, 2343–2346.
- DORCHIES, F., AMIRANOFF, F., BATON, S., BERNARD, D., CROS, B., DESCAMPS, D., JACQUET, F., MALKA, V., MARQUÈS, J.-R., MATTHIEUSSENT, G., MINÉ, PH., MODENA, A., MORA, P., MORILLO, J., NAJMUDIN, Z. & SOLODOV, A. (1999). Electron acceleration in laser wakefield experiments at Ecole Polytechnique. *Laser Part. Beams* **17**, 299–305.
- ESAREY, E., HUBBARD, R.F., LEEMANS, W.P., TING, A. & SPRANGLE, P. (1997). Electron injection into plasma wakefields by colliding laser pulses. *Phys. Rev. Lett.* **79**, 2682–2685.
- EVERETT, M., LAL, A., GORDON, D., CLAYTON, C.E., MARSH, K.A. & JOSHI, C. (1994). Trapped electron acceleration by a laser-driven relativistic plasma wave. *Nature* **368**, 527–529.
- FAURE, J., GLINEC, Y., PUKHOV, A., KISELEV, S., GORDIENKO, S., LEFEBVRE, E., ROUSSEAU, J.-P., BURG, F. & MALKA, V. (2004). A laser-plasma accelerator producing monoenergetic electron beams. *Nature*.
- FRITZLER, S., LEFEBVRE, E., MALKA, V., BURG, F., DANGOR, A.E., KRUSHELNICK, K., MANGLES, S.P.D., NAJMUDIN, Z., ROUSSEAU, J.-P. & WALTON, B. (2004). Emittance measurements of a laser-wakefield-accelerated electron beam. *Phys. Rev. Lett.* **92**, 165006.
- GAHN, C., TSAKIRIS, G.D., PUKHOV, A., MEYER-TER-VEHN, J., PRETZLER, G., THIROLF, P., HABS, D. & WITTE, K.J. (1999). Multi-MeV electron beam generation by direct laser acceleration in high-density plasma channels. *Phys. Rev. Lett.* **83**, 4772–4775.
- HOFFMANN, D.H.H., BLAZEVIC, A., NI, P., ROSMEJ, O., ROTH, M., TAHIR, N.A., TAUSCHWITZ, A., UDREA, S., VARENTSOV, WEYRICH, K. & MARON, Y. (2005). Present and future perspectives for high energy density physics with intense heavy ion and laser beams. *Laser Part. Beams* **23**, 47–53.
- KITAGAWA, Y., MATSUMOTO, T., MINAMIHATA, T., SAWAI, K., MATSUO, K., MIMA, K., NISHIHARA, K., AZECHI, H., TANAKA, K.A., TAKABE, H. & NAKAI, S. (1992). Beat-wave excitation of plasma wave and observation of accelerated electrons. *Phys. Rev. Lett.* **68**, 48–51.
- MALKA, V. (2002). Charged particle source produced by laser-plasma interaction in the relativistic regime. *Laser Part. Beams* **20**, 217–221.
- MALKA, V., FRITZLER, S., LEFEBVRE, E., ALEONARD, M.-M., BURG, F., CHAMBARET, J.-P., CHEMIN, J.-F., KRUSHELNICK, K., MALKA, G., MANGLES, S.P.D., NAJMUDIN, Z., PITTMAN, M., ROUSSEAU, J.-P., SCHEURER, J.-N., WALTON, B. & DANGOR, A.E. (2002). Electron acceleration by a wake field forced by an intense ultrashort laser pulse. *Science* **298**, 1596–1600.
- MALKA, V., FAURE, J., MARQUÈS, J.-R., AMIRANOFF, F., ROUSSEAU, J.-P., RANC, S., CHAMBARET, J.-P., NAJMUDIN, Z. & SOLODOV, A. (2001). Characterization of electron beams produced by ultrashort (30 fs) laser pulses. *Phys. Plasmas* **8**, 2605–2608.
- MODENA, A., DANGOR, A., NAJMUDIN, Z., CLAYTON, C., MARSH, K., JOSHI, C., MALKA, V., DARROW, C., NEELY, D. & WALSH, F. (1995). Electron acceleration from the breaking of relativistic plasma waves. *Nature* **337**, 606–608.
- MOORE, C.I., TING, A., KRUSHELNICK, K., ESAREY, E., HUBBARD, R.F., HAFIZI, B., BURRIS, H.R., MANKA, C. & SPRANGLE, P. (1997). Electron trapping in self-modulated laser wakefields by Raman backscatter. *Phys. Rev. Lett.* **79**, 3909–3912.
- NAKAJIMA, K. (2000). Particle acceleration by ultraintense laser interactions with beams and plasmas. *Laser Part. Beams*, **18**, 519–528.
- PITTMAN, M., FERRÉ, S., ROUSSEAU, J.-P., NOTEBAERT, L., CHAMBARET, J.-P. & CHÉRIAUX, G. (2002). Design and characterization of a near-diffraction-limited femtosecond 100-TW 10-Hz high-intensity laser system. *Appl. Phys. B* **74**, 529–535.
- PUKHOV, A. & MEYER-TER-VEHN, J. (2002). Laser wake field acceleration: the highly non-linear broken-wave regime. *Appl. Phys. B* **74**, 355–361.
- PUKHOV, A. (1999). Three-dimensional electromagnetic relativistic particle-in-cell code VLPL (Virtual Laser Plasma Lab). *J. Plasma Phys.* **61**, 425–433.
- PUKHOV, A., SHENG, Z.-M. & MEYER-TER-VEHN, J. (1999). Particle acceleration in relativistic laser channels. *Phys. Plasmas* **6**, 2847–2854.
- SHOROKOV, O. & PUKHOV, A. (2004). Ion acceleration in overdense plasma by short laser pulse. *Laser Part. Beams* **22**, 175.
- SPRANGLE, P., ESAREY, E., KRALL, J. & JOYCE, G. (1992). Propagation and guiding of intense laser pulses in plasmas. *Phys. Rev. Lett.* **69**, 2200–2203.
- STRICKLAND, D. & MOUROU, G. (1985). Compression of amplified chirped optical pulses. *Opt. Comm.* **56**, 219–221.
- TAHIR, N.A., UDREA, S., DEUTSCH, C., FORTOV, V.E., GRANDJOUAN, N., GRYAZNOV, V., HOFFMANN, D.H.H., HÜLSMANN, P., KIRK, M., LOMONOSOV, I.V., PIRIZ, A.R., SHUTOV, A., SPILLER, P., TEMPORAL, M. & VARENTSOV, D. (2004). Target heating in high-energy-density matter experiments at the proposed GSI FAIR facility: Non-linear bunch rotation in SIS100 and optimization of spot size and pulse length. *Laser Part Beams* **22**, 485–493.
- TAJIMA, T. & DAWSON, J.M. (1979). Laser electron accelerator. *Phys. Rev. Lett.* **43**, 267–270.
- UMSTADTER, D., CHEN, S.-Y., MAKSIMCHUK, A., MOUROU, G. & WAGNER, R. (1996a). Nonlinear optics in relativistic plasmas and laser wake field acceleration of electrons. *Science* **273**, 472–475.
- UMSTADTER, D., KIM, J.-K. & DODD, E. (1996b). Laser injection of ultrashort electron pulses into wakefield waves. *Phys. Rev. Lett.* **76**, 2073–2076.
- WEBER, S., RIAZUELO, G., MICHEL, P., LOUBERE, R., WALRAET, F., TIKHONCHUK, V.T., MALKA, V., OVADIA, J. & BONNAUD, G. (2004). Modeling of laser-plasma interaction on hydrodynamic scales: Physics development and comparison with experiments. *Laser Part. Beams* **22**, 189–195.